Reliable recovery of hierarchically sparse signals and application in machine-type communications

Ingo Roth, Martin Kliesch, Gerhard Wunder, and Jens Eisert

arXiv:1612.07806v2 [cs.IT] 29 Dec 2016

***Abstract*—We examine and propose a solution to the problem of recovering a block sparse signal with sparse blocks from linear measurements. Such problems naturally emerge in the context of mobile communication, in settings motivated by desiderata of a 5G framework. We introduce a new variant of the Hard Thresholding Pursuit (HTP) algorithm [1] referred to as HiHTP. For the specific class of sparsity structures, HiHTP performs significantly better in numerical experiments compared to HTP. We provide both a proof of convergence and a recovery guarantee for noisy Gaussian measurements that exhibit an improved asymptotic scaling in terms of the sampling complexity in comparison with the usual HTP algorithm.**

I. Introduction

An important task in the recovery of signals is to approximately reconstruct a vector $\mathbf{x} \in \mathbb{C}^d$ from m noisy linear measurements

$$\mathbf{y} = \mathbf{A}\mathbf{x} + \mathbf{e} \ \in \mathbb{C}^m, \tag{1}$$

where $\mathbf{A} \in \mathbb{C}^{m\times d}$ is the measurement map and $\mathbf{e} \in \mathbb{C}^m$ denotes additive noise. Such problems arise in many applications, e.g., in image processing, acoustics, radar, machine learning, quantum state tomography, and mobile communication. Particularly interesting is the case where the number of measurements m is much smaller than the dimension of the signal space and where $\mathbf{x}$ has some known structure. The machinery of compressed sensing provides powerful tools for an efficient, stable, and unique reconstruction of $\mathbf{x}$ from $\mathbf{y}$ and $\mathbf{A}$. For many instances, this idea works extraordinarily well and is most prominently investigated for the case where $\mathbf{x}$ is sparse, see ref. [2] and references therein. The most common setting is the one of s-sparse vectors, i.e., vectors that have at most s non-zero entries.

A. Problem formulation

In this work, we investigate a natural setting with more structure than mere s-sparsity in which even superior performance of reconstruction is to be expected: This is the situation in which $\mathbf{x} \in \mathbb{C}^{Nn}$ is partitioned into N blocks each of size n, where at most $\sigma \leq n$ many elements in $s \leq N$ blocks are non-zero. We call vectors of such a sparsity pattern (s, σ)-*sparse*. This structure can be regarded as a simple instance of a larger class of hierarchical sparsity structures which have certain sparsities for nested levels of groupings and has been introduced in refs. [3]–[6]. Hierarchical sparse structures arise in a variety of different applications, see refs. [7]–[9] for recent examples. It can further be seen as a combination of block sparsity [10], [11] and level sparsity [12], [13].

This study is motivated by the desire to identify model-based sparsity structures [14] that (i) allow for efficient, stable and reliable recovery algorithms and (ii) are relevant in concrete technological applications.

B. Application in machine-type communications

One specific application of hierarchical sparse structures that we have in mind is the support of massive machine-type communication (mMTC) traffic in fifth generation (5G) mobile communication systems. Such mMTC traffic is essentially sporadic, i.e. only a few handhelds or devices are actually active out of many, and message sizes are typically small rendering the overall access protocol overhead in current systems (2–4G) infeasibly large [15]. Since, in addition, mMTC devices operate under tight (resource) constraints such as low cost, battery lifetime or computation capability new access protocols have been explored for 5G [16]. In this context compressed sensing was identified as a major tool for rendering 5G access protocols efficient and scalable (see [17] for an overview). More specifically, recent proposals suggest "one-shot" random access concepts where devices wake up and send data right away with no coordination whatsoever [18] combined with a packet collision resolution procedure [19] called *Compressive Coded Random Access*. Here, hierarchical sparse structures naturally emerge when sparse device activity and the (sparse) *channel impulse responses* (CIR) are jointly detected which is now shortly outlined.

CCRA employs a common overloaded control channel to simultaneously detect the activity and CIRs. To this end the i-th user sends a pilot signals $p_i \in \mathbb{C}^w$ into the control channel of bandwidth $w \in \mathbb{N}$. The CIRs with respect to a single user $\mathbf{x}^{(i)} \in \mathbb{C}^n$ can be stacked into a vector $\mathbf{x} \in \mathbb{C}^{Nn}$ allowing for a maximum number of N users. The received signal in an OFDM-type setting has the measurement matrix [18]

$$\mathbf{A} = \Phi \mathcal{F}^{(w)} D(p). \tag{2}$$

The matrix $D(p) \in \mathbb{C}^{w\times Nn}$ depends on the pilot signals $p = [p_1, p_2, \ldots, p_N]$, which the users send as their signature together with the signal. The discrete Fourier transform is

This work was presented at "The First Colloquium on the Priority Programme Compressed Sensing in Information Processing (CoSIP)" in Aachen, Germany, and the "International Traveling Workshop On Interactions Between Sparse Models and Technology, iTWIST" in Aalborg, Denmark, in 2016.

I. Roth and J. Eisert are with the Dahlem Center for Complex Quantum Systems, Freie Universität Berlin, Germany; M. Kliesch is with the Institute for Theoretical Physics, University of Cologne, Germany and the Institute of Theoretical Physics and Astrophysics, University of Gdańsk, Poland; G. Wunder is with the Department of Mathematics and Computer Science, Freie Universität Berlin, Germany. (i.roth@fu-berlin.de)

denoted by $\mathcal{F}^{(w)} \in \mathbb{C}^{w\times w}$ and $\Phi \in \mathbb{C}^{m\times w}$ is a mask selecting only m of the w Fourier coefficients.

The signal modelled by $\mathbf{x}$ will have a specific structure in a cellular communication setup. In a network with a large number of users N having only sporadic traffic, $\mathbf{x}$ will be block-sparse with a number s of maximally simultaneously active users much smaller than N. Furthermore, one observes that the CIR for each user itself is σ-sparse, see ref. [20] and references therein. In this context, it is hence natural to assume that $\mathbf{x}$ is an (s,σ)-sparse signal as introduced above.

The precise form of the measurement matrix $\Phi\mathcal{F}^{(w)}D(p)$ depends on the construction of the pilot signal which are often Zhadoff-Chu sequences [18]. The main requirement in the classical context is that these sequences remain orthogonal under circular time shift. To be concise for the moment, we only consider the case where the length of the CIRs n is smaller than or equal to the available bandwidth per user w/N. Without loss of generality, we set $w = qnN$ with $q \in \mathbb{N}$. In fact, this restriction allows for the following construction of the pilot signals: We choose the Fourier transform of p_1 to be of the form $\hat{p}_1 = [\mathrm{e}^{2\pi\mathrm{i}\omega_1}, \mathrm{e}^{2\pi\mathrm{i}\omega_2}, \dots, \mathrm{e}^{2\pi\mathrm{i}\omega_w}]^T$ with random phases ω_i in $[0,1)$. The pilot signals of the other users can be choosen such that $D(p) = \operatorname{circ}(p_1)_{[Nn]}$, i.e. the first nN columns of the circulant matrix generated by p_1. Therefore, the measurement matrix takes the form

$$\mathbf{A} = \Phi \operatorname{diag}(\hat{p}_1)\mathcal{F}^{(w)}_{[Nn]}, \tag{3}$$

where we have used that the Fourier transform of a circulant matrix fulfills $\mathcal{F}^{(w)} \operatorname{circ}(p_1) = \operatorname{diag}(\hat{p}_1)\mathcal{F}^{(w)}$. We observe that in our setting the measurements are partial Fourier measurements in a larger ambient dimension with additionally random phases. In addition, we can make the following simplification: Firstly, since the random phases are known as part of the measurement matrix, we can multiply the samples $\mathbf{y}$ elementwise by the inverted phases at the beginning of the reconstruction. Thus, it is sufficient to consider the trivial case $\operatorname{diag}(\hat{p}_1) = \mathrm{Id}$. Secondly, we have some freedom to design the mask Φ selecting the measured Fourier coefficients. By sampling uniformly from the equidistant set $\{1, q+1, 2q+1, 3q+1, \dots, (nN-1)q+1\}$, we reduce the restriction of the w-dimensional discrete Fourier transform to an unrestricted nN-dimensional Fourier transform, i.e.,

$$\Phi\mathcal{F}^{(w)}_{[Nn]} = \tilde{\Phi}\mathcal{F}^{(Nn)} \tag{4}$$

with a mask $\tilde{\Phi}$ selecting a support drawn uniformily from $[Nn]$. In summary, the task of channel estimation and user activity detection requires the reconstuction of a (s,σ)-sparse vector $\mathbf{x}$ from linear measurements. In our setting the measurements are simply partial Fourier measurement

$$\mathbf{A} = \tilde{\Phi}\mathcal{F}^{(Nn)}. \tag{5}$$

C. Contributions of this work

We identify the sparsity structure, namely (s,σ)-sparsity, appearing in multiuser, multipath communication settings and provide a concrete example within the CCRA protocol. In this concrete application the measurement matrix takes the simple form of a partial Fourier measurement matrix. We propose a new efficient algorithmic solution for the recovery of hierarchical sparse problems and provide a stable and robust recovery guarantee based on generalised RIP conditions. For Gaussian measurements we provide RIP bounds for a large class of hierarchical sparsity patterns including the simple case of (s,σ)-sparsity. Therefore, the proposed algorithm has an improved sampling complexity compared to standard CS approaches. The algorithm is compared to standard CS algorithms and convex optimisation techniques for hierarchical sparse structures. For Gaussian and partial Fourier measurements an improved sampling complexity is found numerically for the proposed algorithm.

D. Related work

Sparse user activity in MTC as well as sparse channel esimation has been meanwhile studied in many works, see [17]. Both sparsity features can be separately exploited with standard compressed sensing algorithms, e.g., ℓ_1-norm optimisation [20], [21]. However, the combined sparsity structure arising from sparse CIRs in a scheme with sporadic traffic was not investigated to the knowledge of the authors.

This work follows the outline of model based compressed sensing [14] and makes use of generalised RIP constants for unions of finite-dimensional linear subspaces as proposed in ref. [22]. The structure of hierarchically sparse signals can be seen as a combination of level sparsity [12], [13] and block sparsity [10], [11]. In the latter body of work it has been pointed out that block-sparse signals can be recovered by minimising the mixed norm $\|\cdot\|_{\ell_2/\ell_1}$ which amounts to the sum of the ℓ_2-norms of the blocks. Also, corresponding block thresholding algorithm have been proposed, such as Group Orthorgonal Matching Pursuit [23].

The notion of hierarchical sparsity and the special case of block sparse vectors with sparse blocks has been introduced in refs. [3]–[6]. Herein a linear combination of the ℓ_1-norm and the mixed ℓ_2/ℓ_1-norm is employed as a regulariser for (s,σ)-sparse signals. The resulting convex optimisation problem reads as

$$\text{minimise } \frac{1}{2}\|\mathbf{y} - \mathbf{A}\mathbf{x}\|^2 + \mu\|\mathbf{x}\|_{\ell_1} + \lambda\|\mathbf{x}\|_{\ell_2/\ell_1}. \tag{6}$$

The iterative soft thresholding algorithm solving this optimisation problem was dubbed HiLasso. For HiLasso convergence and recovery guarantees have been shown based on generalised notions of coherence for the block-sparse structure. To the authors' knowledge there are no results available on the required sampling complexity for specific ensembles of measurement matrices such as Gaussian measurements to fulfill the coherence conditions. A generalisation of the Orthogonal Matching Pursuit algorithm to (s,σ)-sparse vectors has been proposed in ref. [24] providing only numerical indications of its performance. In refs. [25]–[27] generalisations of the regulariser of (6) have been constructed to reconstruct signals with more general sparsity structures that involve groupings of vector entries.

E. Notation

The set of positive integers being not larger than $n \in \mathbb{Z}^+$ is denoted by $[n] := \{1, 2, \dots, n\}$. By $\mathbb{K}$ we denote a field that is either the real numbers $\mathbb{R}$ or the complex numbers $\mathbb{C}$. The imaginary unit is denoted by i so that $\mathrm{i}^2 = -1$. The ℓ_q-norm of $\mathbf{x} \in \mathbb{K}^d$ is denoted by $\|\mathbf{x}\|_{\ell_q} := (\sum_j |x_j|^q)^{1/q}$ and the Euclidean norm by $\|\mathbf{x}\| := \|\mathbf{x}\|_{\ell_2}$. With $\mathrm{supp}(\mathbf{x}) := \{j : x_j \neq 0\}$ we denote the support of a vector $\mathbf{x} \in \mathbb{K}^d$.

Given a matrix $\mathbf{A} \in \mathbb{K}^{m \times d}$ we refer by $\mathbf{A}_\Omega$ with $\Omega \subset [d]$ to the $m \times |\Omega|$ *submatrix* consisting only of the columns indicated by Ω. Analogously, for a vector $\mathbf{x} \in \mathbb{K}^d$ the *restriction* to Ω is denoted $\mathbf{x}_\Omega \in \mathbb{K}^{|\Omega|}$. We write $\mathbf{x}|_\Omega$ for the *projection* of $\mathbf{x}$ to the subspace of $\mathbb{K}^d$ with support Ω, i.e.

$$(\mathbf{x}|_\Omega)_k := \begin{cases} x_k & \text{for } k \in \Omega, \\ 0 & \text{for } k \notin \Omega. \end{cases} \tag{7}$$

Furthermore, the complement of $\Omega \subset [d]$ is denoted by $\bar{\Omega} := [d] \setminus \Omega$.

II. The Algorithm: HiHTP

Established thresholding and greedy compressed sensing algorithms, e.g., CoSaMP [28] and Hard Thresholding Pursuit (HTP) [1], follow a common strategy: In each iteration, first, a proxy to the signal $\mathbf{x}$ is computed from the previous approximation to the signal and from the measurement vector $\mathbf{y}$. From this proxy a guess for the support of $\mathbf{x}$ is inferred by applying a thresholding operation. As a second step of the iteration, the best ℓ_2-norm approximation to the measurements compatible with this support is calculated.

In HTP the s-sparse thresholding operator (TO) $L_s : \mathbb{C}^n \to \{\Omega \subset [n] \mid |\Omega| = s\}$ is given by

$$L_s(\mathbf{z}) := \{\text{indices of } s \text{ largest entries of } \mathbf{z} \text{ in magnitude}\}.$$

This operator returns the support $L_s(\mathbf{z}) \subset [d]$ of the best s-sparse approximation to $\mathbf{z}$. The basic idea of model-based compressed sensing [14] is to adapt this TO to the model in order to improve the performance of the algorithm. We denote the TO that yields the support of the best (s, σ)-sparse approximation to $\mathbf{z} \in \mathbb{C}^{nN}$ by $L_{s,\sigma}$. Importantly, in this case, $L_{s,\sigma}(\mathbf{z})$ can be easily calculated: We apply the σ-sparse TO to each block separately, select the s active blocks as the largest truncated blocks in ℓ_2-norm, and collect the remaining $s \cdot \sigma$ indices in the set $L_{s,\sigma}(\mathbf{z})$. This prescription is illustrated in Figure 1.

Using $L_{s,\sigma}$ instead of L_s in the HTP yields Algorithm 1, which we call HiHTP, as it is designed to recover a *hi*erarchically structured sparsity. As in the original HTP proposal, a natural stopping criterion is that two subsequent supports coincide, i.e. $\Omega^{k+1} = \Omega^k$.

A similar modification employing $L_{s,\sigma}$ can also be applied to other compressed sensing algorithms including Iterative Hard Thresholding [29], Subspace Pursuit [30] or Orthorgonal Matching Pursuit, see e.g., ref. [31] and references therein.

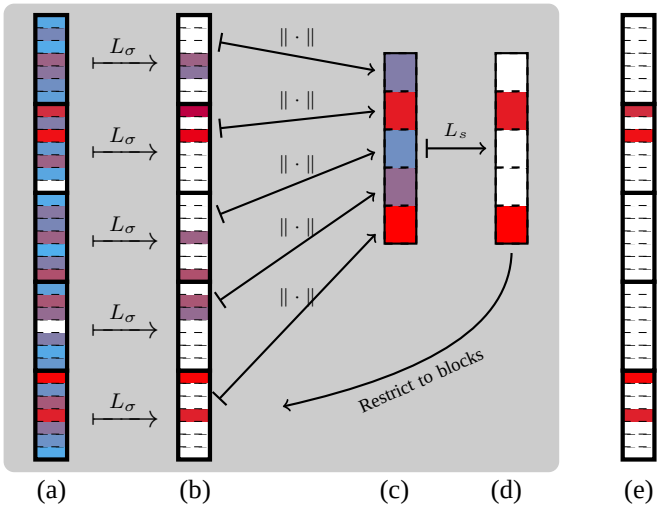

Figure 1. In this figure, the evaluation of the hierarchical thresholding operator $L_{s,\sigma}$ is illustrated. Starting with a given dense vector (a), each block is thresholded to the best σ-sparse approximation (b). To determine the s dominant blocks, the ℓ_2-norm is calculated for each block. The resulting vector (c) of length N is again thresholded to its best s-sparse approximation (d). The resulting blocks indicated by the s-sparse approximation (d) are selected from the σ-sparse approximation (b). The remaining (s, σ)-sparse support (e) is the output of $L_{s,\sigma}$.

Algorithm 1 (HiHTP)

Input: measurement matrix $\mathbf{A}$, measurement vector $\mathbf{y}$, block column sparsity (s, σ)

1: $\mathbf{x}^0 = 0$
2: **repeat**
3: $\quad \Omega^{k+1} = L_{s,\sigma}(\mathbf{x}^k + \mathbf{A}^*(\mathbf{y} - \mathbf{A}\mathbf{x}^k))$
4: $\quad \mathbf{x}^{k+1} = \arg\min_{\mathbf{z} \in \mathbb{C}^{Nn}} \{\|\mathbf{y} - \mathbf{A}\mathbf{z}\|, \ \mathrm{supp}(\mathbf{z}) \subset \Omega^{k+1}\}$
5: **until** stopping criterion is met at $\tilde{k} = k$

Output: (s, σ)-sparse vector $\mathbf{x}^{\tilde{k}}$

Computational complexity: The computational complexity of HiHTP scales identical as for the original HTP. The algorithms only differ in the thresholding operators. Using a quickselect algorithm [32] to perform the thresholding operator yields computational costs of $\mathcal{O}(Nn)$ for both algorithms.

The overal performance is dominated by the costs of matrix vector multiplication with the measurement matrix $\mathbf{A}$ and $\mathbf{A}^*$, e.g., for the calculation of the proxy. Therefore the computation time in general scales as $\mathcal{O}(mNn)$. If the measurement matrix allows for a fast matrix vector multiplication this scaling can be improved [28].

III. Analytical Results

For the analysis of hierarchically sparse recovery schemes, we use a special version of the general restricted isometry property (RIP) for unions of linear subspaces [22]. In the following we formulate the RIP for (s, σ)-sparse vectors. A generalised version for arbitrary hierachical sparse vectors is given in Section V.

Definition 1 (RIP)**.** Given a matrix $\mathbf{A} \in \mathbb{K}^{m \times nN}$, we denote

by $\delta_{s,\sigma}$ the smallest $\delta \geq 0$ such that

$$(1-\delta)\|\mathbf{x}\|^2 \leq \|\mathbf{A}\mathbf{x}\|^2 \leq (1+\delta)\|\mathbf{x}\|^2 \tag{8}$$

for all (s,σ)-sparse vectors $\mathbf{x} \in \mathbb{K}^{nN}$.

Since every (s,σ)-sparse vector is $s\cdot\sigma$-sparse, we immediately observe that $\delta_{s,\sigma} \leq \delta_{s\cdot\sigma}$. Furthermore, the (s,σ)-sparse RIP constants are non-decreasing in both their indices,

$$\begin{aligned} \delta_{s,\sigma} &\leq \delta_{s+1,\sigma}\,, \\ \delta_{s,\sigma} &\leq \delta_{s,\sigma+1} \end{aligned} \tag{9}$$

for all s and σ.

The $s\cdot\sigma$-sparsity of (s,σ)-sparse vectors allows to apply standard compressed sensing algorithms for the recovery from linear measurements for which recovery guarantees have been shown. Due to the their similarity, HiHTP inherits the results for the success of recovery for measurement matrices with small RIP constants that have been established for HTP [1]. See also ref. [2, Chapter 6.3].

The RIP condition on the measurement matrix derived therein is $\delta_{3s} < 1/\sqrt{3}$.

One main technical insight of model-based compressed sensing [14] is that the generalised RIP of ref. [22] allows for the same proof techniques as the standard RIP [33] and leads to improved recovery guarantees. Following this strategy, we can establish less restrictive RIP-type conditions for successful recovery in terms of the custom tailored (s,σ)-sparse RIP constants. The resulting statement is the following:

Theorem 1 (Recovery guarantee)**.** *Suppose that the following RIP condition holds*

$$\delta_{3s,2\sigma} < \frac{1}{\sqrt{3}}. \tag{10}$$

Then, for $\mathbf{x} \in \mathbb{C}^{nN}$, $\mathrm{e} \in \mathbb{C}^m$, and $\Omega \subset [n]\times[N]$ a (s,σ)-sparse support set, the sequence (x^k) defined by HiHTP *(Algorithm 1) with $\mathbf{y} = \mathbf{A}\mathbf{x}\rfloor_\Omega + \mathbf{e}$ satisfies, for any $k \geq 0$,*

$$\left\|\mathbf{x}^k - \mathbf{x}\rfloor_\Omega\right\| \leq \rho^k \left\|\mathbf{x}^0 - \mathbf{x}\rfloor_\Omega\right\| + \tau\left\|\mathbf{e}\right\|, \tag{11}$$

where

$$\rho = \left(\frac{2\delta_{3s,2\sigma}}{1-\delta_{2s,2\sigma}^2}\right)^{1/2} < 1 \tag{12}$$

and $\tau \leq 5.15/(1-\rho)$.

The complete proof is given in Appendix A. The proof proceeds verbatim along the lines of the proof of the convergence result for HTP [1], [2]. The modified thresholding operator $L_{s,\sigma}$ can be treated analogously to standard thresholding operator in the original proof. The main difference is that while the proof for HTP uses standard RIP constants to bound the deviation of the algorithm's output $\mathbf{x}^k$ from the original signal $\mathbf{x}_\Omega$, we are in a position to employ the (s,σ)-spares RIP constants in these bounds for HiHTP. The crucial observation regarding the generalised RIP constants is the following.

Observation 2 (Support unions)**.** *For $i = 1,2$ let $\Omega_i \subset [N]\times[n]$ be an (s_i,σ_i)-sparse support and $\mathbf{A} \in \mathbb{K}^{m\times Nn}$ with RIP constants $\delta_{s,\sigma}$. Then*

$$\|\mathrm{Id} - (\mathbf{A}_{\Omega_1\cup\Omega_2})^*\mathbf{A}_{\Omega_1\cup\Omega_2}\| \leq \delta_{s_1+s_2,\sigma_1+\sigma_2}. \tag{13}$$

The statement follows directly from hierarchy (9) of the (s,σ)-sparse RIP constants and the observation that the union $\Omega_1\cup\Omega_2$ has at most s_1+s_2 blocks and each block is at most $\sigma_1+\sigma_2$ sparse.

In fact, one can prove an alternative bound replacing the right hand side of (13) by $3\max\{\delta_{s_{\max},\sigma_1+\sigma_2}, \delta_{s_1+s_2,\sigma_{\max}}\}$, where $s_{\max} := \max\{s_1,s_2\}$ and $\sigma_{\max} := \max\{\sigma_1,\sigma_2\}$. The latter bound uses smaller RIP constants compared to Observation 2. However, for Gaussian measurements the formulation of Observation 2 will lead slightly smaller constants. This observation allows to bound terms involving the sum of two and more (s,σ)-sparse vectors. Employing this in the proof of Theorem 1 yields the modified RIP condition (10).

The trivial bound $\delta_{2s,2\sigma} \leq \delta_{4s\sigma}$ does not indicate an improvement by the theorem compared to the established bound $\delta_{3s} < 1/\sqrt{3}$. But the decreased number of subspaces which contribute to (s,σ)-sparse vectors compared to the set of all $s\sigma$-sparse vectors allows us to provide tighter bounds for $\delta_{s,\sigma}$ compared to $\delta_{s\sigma}$ for specific random matrices. Building on [22, Theorem 3.3.], we establish the following result for the case of real Gaussian measurement matrices.

Theorem 3 ((s,σ)-sparse RIP for real Gaussian measurements)**.** *Let $\mathbf{A}$ be an $m\times(N\cdot n)$ real matrix with i.i.d. Gaussian entries and $m < Nn$. For $\epsilon > 0$, assume that*

$$m \geq \frac{36}{7\delta}\left(s\ln\left(\frac{\mathrm{e}N}{s}\right) + s\sigma\ln\left(\frac{\mathrm{e}n}{\sigma}\right) + \ln\left(\frac{12}{\delta}\right) + \ln(\epsilon^{-1})\right). \tag{14}$$

Then, with probability of at least $1-\epsilon$, the restricted isometry constant $\delta_{s,\sigma}$ of $\mathbf{A}/\sqrt{m}$ satisfies

$$\delta_{s,\sigma} \leq \delta. \tag{15}$$

Proof: The bounds on RIP constants for typical random matrices, e.g., Gaussian matrices or matrices with sub-Gaussian rows, proceed in two steps, see e.g., ref. [2, Chapter 9]. From the properties of the specific random measurement matrix they derive a bound on the probability that $\|\mathbf{A}\mathbf{x}\|^2 - \|\mathbf{x}\|^2 \leq \epsilon\|\mathbf{x}\|^2$ for a fixed $\mathbf{x}$. With such a bound the RIP constant can be upper bounded by taking the union bound over all relevant subspaces that might contain $\mathbf{x}$. For example, for the standard RIP constant δ_s for s-sparse vectors in $\mathbb{R}^n$ one has to consider the $\binom{n}{s}$ subsets of $[n]$ with cardinality s. In this way, one establishes a bound on δ_s to hold with high probability provided that the number of samples of the measurement matrix is lower bounded, $m \geq \tilde{m}$, with $\tilde{m} \in \mathcal{O}\big(s\ln(n/s)\big)$.

The general formulation for RIP constants of Gaussian matrices for vectors of union of subspaces was derived in ref. [22]. Theorem 3 is a direct corollary of the result of ref. [22] applied to (s,σ)-sparse vectors. Theorem 3.3. of ref. [22] establishes that a i.i.d. Gaussian matrix $\mathbf{A} \in \mathsf{R}^{m\times d}$ has the RIP property with RIP constant upper bounded by δ with respect to vectors of a union of L k-dimensional subspaces with probability of $1-\epsilon$ provided that

$$m \geq \frac{36}{7\delta}\left(\ln(2L) + k\ln\left(\frac{12}{\delta}\right) + \ln\epsilon^{-1}\right). \tag{16}$$

An (s,σ)-sparse signal is in the union of

$$\binom{N}{s}\binom{n}{\sigma}^{\sigma} \leq \left(\frac{eN}{s}\right)^{s}\left(\frac{en}{\sigma}\right)^{s\sigma} \tag{17}$$

one-dimensional subspaces. Thus, (16) yields the statement of Theorem 3 for the case of (s,σ)-sparse vectors. ∎

Combining Theorem 1 and Theorem 3, we establish the successful recovery of (s,σ)-sparse vectors from Gaussian measurements provided that the number of samples $m \geq \tilde{m}$, where the lower bound on the number of samples $\tilde{m}$ parametrically scales like

$$\tilde{m} \in \mathcal{O}\big(s\ln(N/s) + s\sigma\ln(n/\sigma)\big). \tag{18}$$

For Gaussian measurements the standard RIP analysis of HTP in our setting yields recovery guarantees for a number of samples $m \geq \tilde{m}$ with parametric scaling $\tilde{m} \in \mathcal{O}\big(s\sigma\ln(Nn/(s\sigma))\big)$, see, e.g., ref. [2]. Compared to this well-known scaling the HiHTP requires parametrically $s(\sigma-1)\ln(N/s)$ fewer samples for guaranteed successful recovery.

For the direct application to the CCRA protocol similar improved bounds for subsampled Fourier matrices are required. However, the different proof techniques render the adaption of such bounds to hierarchical sparse signals more difficult. We leave analytic results for the recovery of hierarchical sparse signals from partial Fourier measurements to future work. In the next section we find numerically similar results for Gaussian measurements and partial Fourier measurements.

IV. Numerical results

In this section we compare the performance of HiHTP, HTP and the HiLasso-algorithm in numerical experiments for Gaussian and Fourier measurements.

All algorithms have been implemented in Matlab [34]. For the implementation of HiLasso the convex optimisation problem (6) was directly solved using CVX [35] with MOSEK [36] to avoid ambiguities in the implementation of the soft-thresholding algorithm. Before the HTP and HiHTP algorithms are applied the columns of the measurement matrix are normalised in ℓ_2-norm. The entries of the result of the algorithms are subsequently multiplied by the normalising factors to restore the ℓ_2-norms of the columns of the actual measurement matrix.

A. Block recovery rates

In compressed sensing a common performance measure is the fraction of recovered signals given a certain amount of samples to quantify the performance of an algorithm in solving a linear inverse problem (1). In the context of block-structured signals there is a different measure of performance available, which is well motivated in multiple applications, e.g., in OFDM. We consider a *block* recovered if the reconstructed part of the signal deviates from the original signal by less than ϵ in ℓ_2-norm. The choice of ϵ depends on the specific application and, in particular, its noise model. For a given number of samples we count the total number of recovered blocks. Furthermore, we distinguish between the number of recovered blocks which are non-zero and of those which are zero in the original signal.

B. Gaussian measurements

We consider $(s=4,\sigma=20)$-sparse signals consisting of $N=30$ blocks of dimension $n=100$. For each instance of the signal the supports are randomly drawn from a uniform distribution and the entries are i.i.d. real numbers from a standard normal distribution. We subsequently run HTP, HiHTP and HiLasso on Gaussian measurements of each signal. For different numbers of measurements, we count the number of successfully recovered signals out of 100 runs. A signal is successfully recovered if it deviates by less than 10^{-5} in Euclidean norm from the original signal. This choice is motivated by the observation that deviation is typically either significantly smaller or significantly larger than this value of 10^{-5}.

While it is straightforward to inform the HTP and HiHTP algorithm about the sparsity of the signal, the HiLasso is calibrated by adjusting the weights μ and λ in front of the regulariser terms in (6). We have found that finding appropriate values for both weights requires extensive effort, especially in the presence of additive noise. In applications where the sparsity levels are approximately known hard-thresholding algorithms do not require additional calibration.

For noiseless Gaussian measurements, we have found numerically that HiLasso yields good recovery rates for $\mu=0.4$ and $\lambda=0.5$ in our setting, see Appendix B. Therefore these parameters are used for HiLasso in the tests. The results of all three algorithm are shown in Figure 2.

It often not required to reconstruct the entire signal in an application. Moreoften, a relevant measure of performance is the number of successfully recovered blocks. In the following, a block is successfully recovered if it deviates by less than 10^{-5} in Euclidean norm from the corresponding block of the original signal. For each number of measurements we average the number of recovered blocks over 100 runs.

Figure 3 shows the resulting recovery rates. While for HTP the number of recovered blocks quickly decays for small numbers of samples, HiHTP performs significantly better in this regime. Note that the minimal number of not recovered blocks is lower bounded by $2s$, which follows directly from the definition of HiHTP. Furthermore, the HiHTP recovers the content of the active blocks accurately using less measurements then HTP. The HiLasso algorithm shows a similar behaviour as the HTP algorithm but requires even more samples to achive comparable recovery rates.

The better performance of HiHTP compared to HTP can also be obseverd if Gaussian noise is added to the measurement vector. The block recovery rates for different numbers of samples and signal-to-noise ratios (SNR) of 10^5 and 10^2 are shown in Figure 4. We require a succesfully recovered block to deviate by less than 10^{-2} in Euclidean norm from the corresponding block of the original signal. For SNR $=10^2$ the noise prohibits the accuarate recovery of the active blocks for both algorithms. But for HiHTP the correct identification of the zero blocks can still be archieved. Figure 5 shows the mean distance in Euclidean norm of the reconstructed blocks from the original blocks of the signal.

Table I displays the run times per reconstruction of the HTP and HiHTP algorithm on desktop hardware (2 x 2,4 GHz

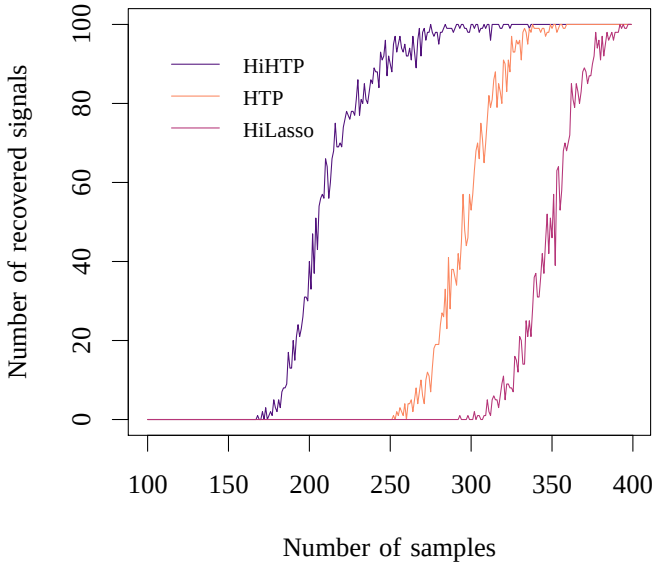

Figure 2. Number of recovered signals from 100 Gaussian samples over the number of measurements m for HTP, HiLasso and HiHTP, the latter introduced here. The signals consist of $N = 30$ blocks of size $n = 100$ with $s = 4$ blocks having $\sigma = 20$ non-vanishing real entries.

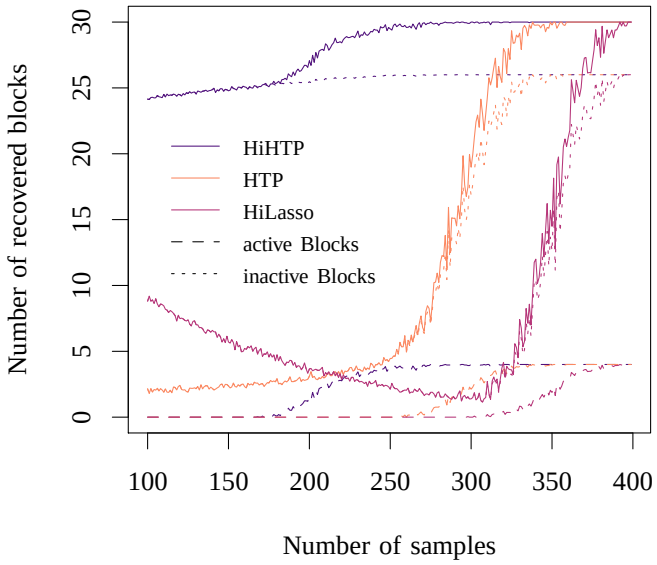

Figure 3. Number of recovered blocks over the number of measurements m for HTP and HiHTP. The dashed and dotted lines indicate the average number of correctly recovered zero and non-zero blocks, respectively. The solid lines show the total average number of recovered blocks. The signals consist of $N = 30$ blocks with $s = 4$ blocks having non-vanishing real entries.

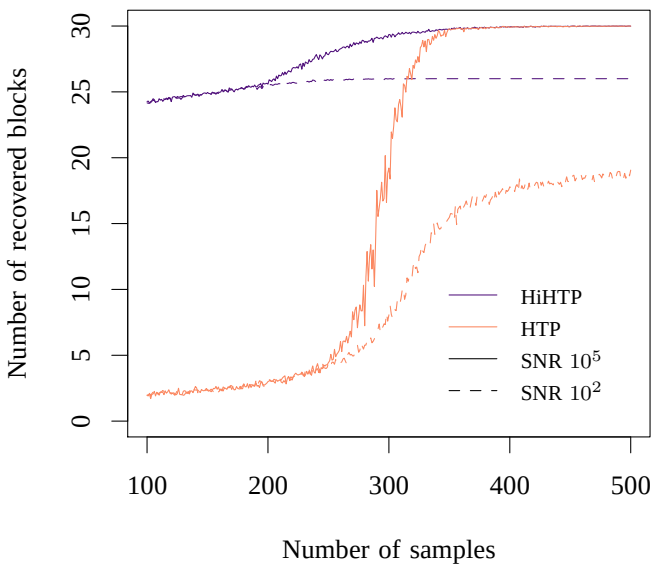

Figure 4. Number of recovered blocks over the number of measurements m for HTP and HiHTP in the presence of additive Gaussian noise. The solid line and dashed lines indicate the number of recovered blocks for an SNR of 10^5 and 10^2, respectively. The signals consist of $N = 30$ blocks with $s = 4$ blocks having non-vanishing real entries.

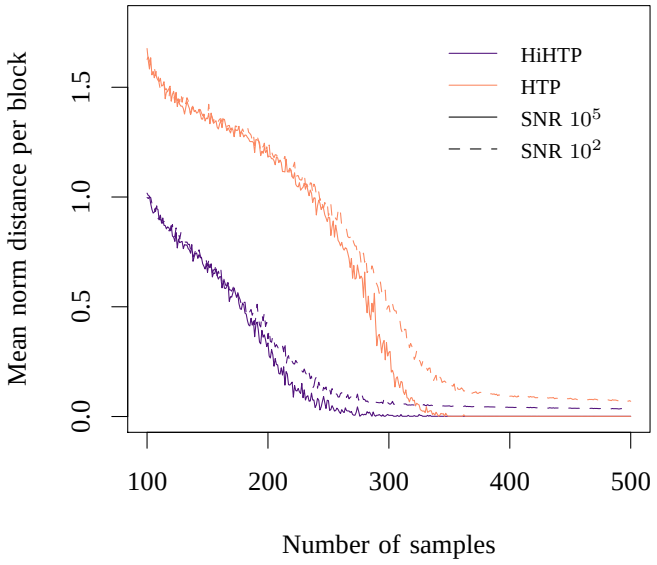

Figure 5. The mean distance of the reconstructed blocks from the original blocks of the signal in Euclidean norm over the number of measurements m for HTP and HiHTP in the presence of additive Gaussian noise. The solid line and dashed lines indicate the number of recovered blocks for anSNR of 10^5 and 10^2, respectively. The signal model has dimensions $N = 30$, $n = 100$, $s = 4$ and $\sigma = 20$.

Table I
RUN TIMES PER RECONSTRUCTION IN SECONDS OF HTP AND HIHTP ON DESKTOP HARDWARE FOR DIFFERENT NUMBERS OF MEASUREMENTS m.

m	200	300	400
HTP	0.29s	0.35s	0.42s
HiHTP	0.34s	0.37s	0.40s

Quad-Core Intel Xeon, 64 GB 1066 MHz DDR3 ECC) in the tests with noiseless Gaussian measurements. The run times are average values of 100 iterations. Both HTP and HiHTP show comparable run times.

C. Fourier measurements

In the application to CCRA one aims at recovering (s, σ)-sparse complex vectors from partial Fourier measurements (5). Figure 6 shows the number of successfully recovered blocks from uniform randomly selected Fourier coefficients for HiHTP and HTP.

An $(s = 3, \sigma = 10)$-sparse support is drawn uniformly of $N = 20$ blocks of dimension $n = 50$. The signal entries are complex numbers with real and imaginary part i.i.d. sampled from a standard normal distribution. Recovery rates are again averaged over 100 runs. Running HiHTP on random partial Fourier measurements shows a qualitatively similar behaviour as for Gaussian measurements.

When we select only the m lowest Fourier coefficients instead of an uniformly sampled subset, we observe that the block support is still recovered from a small amount of samples. In contrast, a correct reconstruction of the content of the active blocks requires a comparatively large amount of samples. Both algorithm HiHTP and HTP perform approximately the same using the lowest Fourier modes (not shown in the figures).

This observation is in agreement with the intuition that the lowest Fourier modes encode information over the large scale structure of the signal. The information whether a block is active or not can be regarded as a property which does not require to resolve the scale of every entry but only larger blocks of the signal. On the contrary, information on the entries inside a block are encoded in the higher Fourier modes.

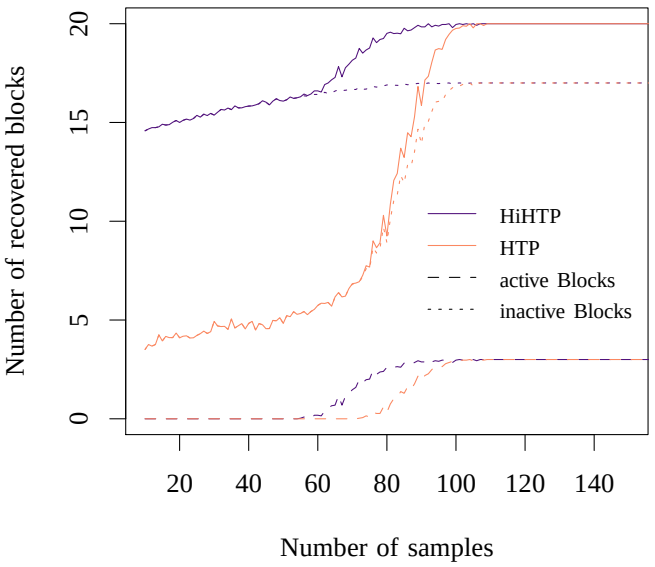

Figure 6. Number of recovered blocks over the number of measurements m for HTP and HiHTP employing uniformly random partial Fourier measurements. The dashed and dotted lines indicate the average number of correctly recovered zero and non-zero blocks, respectively. The solid lines show the total average number of recovered blocks. The signals consist of $N = 20$ blocks with $s = 3$ blocks having non-vanishing real entries.

V. GENERAL HIERARCHICAL SPARSITY

In this section, we provide the general definition of hierarchical sparse vectors that can be efficiently constructed following the strategy of HiHTP. The sparsity structure can have the general hierarchy of an arbitrary rooted tree, possibly with different block sizes and corresponding sparsities. We sketch the corresponding algorithm and give a general version of the recovery results of Section III.

A. Setting and notation

We consider a rooted tree $T = (V, E)$ with vertex set V and edges E. Figure 7 illustrates the following definitions. We denote the root element by $v_0 \in V$. Since the root implies an ordering of the vertices away from the root we get the common notions of the *parent*, *children* and *siblings* of the tree. We denote the parent node of v by $\mathrm{parent}(v) \in V$ and set of its children by $\mathrm{children}(v) \subset V$. Furthermore, the subset of V that has no children are called $\mathrm{leaves}(T)$. We denote the number of leaves of T by $d := |\mathrm{leaves}(T)|$. Let $\mathrm{depth}(v)$ be the length of the unique path from v to v_0. Without loss of generality, we hereinafter require that $\mathrm{depth}(v) = l$ for all $v \in \mathrm{leaves}(T)$ with some constant l. An arbitrary tree can be completed to a tree with constant depth of leaves by attaching a chain of only children to the leaves until a constant depth is achieved. In addition, we assume that the tree is ordered, i.e., there exist an ordering $v < w$ among different siblings v and w. We canonically extend this ordering to all vectices of the same depth by requiring that two vertices with different parent vertices inherit the ordering of their parents.

We define the map $\mathbf{n} : V \to \mathbb{N}$ to count the number of children of a given vertex, i.e. $\mathbf{n}(v) := |\mathrm{children}(v)|$. A *hierarchical support* on T is a map $\mathbf{\Omega} : V \to \mathcal{P}([d])$ such that for all $v \in V$

1) $\mathbf{\Omega}(v) \subset \mathcal{P}([\mathbf{n}(v)])$.

Furthermore, we require that if $\mathbf{\Omega}(v) \neq \emptyset$ then

2) $\mathbf{\Omega}(\mathrm{parent}(v)) \neq \emptyset$
3) and $\exists w \in \mathrm{children}(v) : \mathbf{\Omega}(w) \neq \emptyset$.

Here $\mathcal{P}(M)$ is the power set of a set M. The first condition ensures that at each vertex a subset of indices is selected that can be identified with the children of the vertex using the ordering among siblings. In this way, the map $\mathbf{\Omega}$ assigns to each vertex a subset of its children. We call a vertex v with index in $\mathbf{\Omega}(\mathrm{parent}(v))$ *active in* $\mathbf{\Omega}$. The second and third

condition imply that each active vertex is part of at least one chain of connected active vertices with one vertex at each depth. This requirement ensures that the support on the leaves of T uniquely determines the support on the entire vertex set V. This hierarchical arrangement of the support allows for the identifications of a hierarchical support on T with the support $\Omega \subset [d]$ of a vector $\mathbf{x} \in \mathbb{K}^d$.

In more detail, since the ordering among the siblings was completed to an ordering of all vertices of common depth, we can also assign to an vertex its index among all other vertices of the same depth. In this way, the leaves of T are identified with $[d]$. The groups of siblings in T define a hierarchy of nested blocks of the vector $\mathbf{x} \in \mathbb{K}^d$. The entries of the vector are grouped into blocks as the leaves are grouped into siblings of a parent by T. These blocks are again grouped into larger blocks specified by the ancenstry of the parents of the leaves and so on.

We say $\mathbf{x}$ is *supported on* $\boldsymbol{\Omega}$ if its support Ω coincides with the set of indices of the active leaves of T in $\boldsymbol{\Omega}$. Hence, the blocks of $\mathbf{x}$ with non-vanishing entries are the active vertices of the support map $\boldsymbol{\Omega}$.

Now we would like to allow only a certain number of vertices to be active among siblings for each vertex, corresponding to a restriction of the number of blocks with non-vanishing entries. To this end, we define a *sparsity* on T as a map $\mathbf{s} : V \to \mathbb{N}$ with $\mathbf{s}(v) \leq \mathbf{n}(v)$ for all $v \in V$. A vector support Ω or the corresponding support on the tree $\boldsymbol{\Omega}$ is called $\mathbf{s}$-sparse if $|\boldsymbol{\Omega}(v)| \leq \mathbf{s}(v)$ for all $v \in V$.

B. Algorithm and recovery guarantees

To recover an $\mathbf{s}$-sparse vector $\mathbf{x}$ with block structure given by a tree T from linear measurements we can employ the strategy of HiHTP, Algorithm 1, and generalise the (s, σ)-sparse thresholding operator $L_{s,\sigma}$ to the $\mathbf{s}$-sparse structure.

Given an arbitrary vector $\mathbf{z} \in \mathbb{K}^d$. We assign to each leave of T the corresponding vector entry. The $\mathbf{s}$-sparse thresholding operator $L_{\mathbf{s}}$ starts on the level of the leaves and applies for each block of siblings the standard thresholding operator $L_{\mathbf{s}(v)}$, where v is the parent of the respective block. Subsequently,

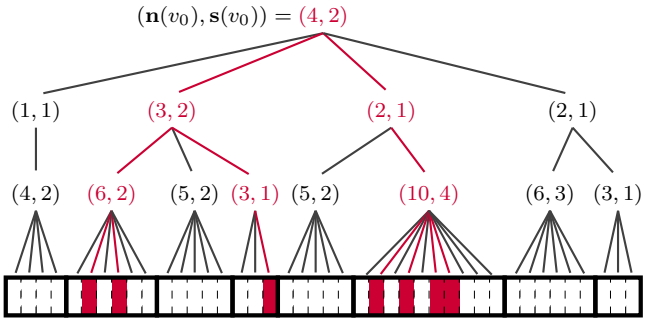

Figure 7. In this figure, an example of a hierarchical sparse vector is given. The grouping of the entries is encoded in a rooted tree. The children of a vertex constitute a block at their level. The pair of values $(\mathbf{n}(v), \mathbf{s}(v))$ is indicated at each vertex. The leaves of the tree are identified with the entries of the vector. The support of the vector and active vertices are highlighted in red.

the ℓ_2-norm of the remaining entries of the block is calculated and assigned to v. Now, we can repeat these two steps by applying $L_{\mathbf{s}(\operatorname{parent} v)}$ to v and all its siblings and assigning the ℓ_2-norm of the remaining vertices to $\operatorname{parent} v$. In this manner, we recursevly select vertices of each level of the tree compatible with condition of $\mathbf{s}(v)$-sparsity. At a final step, we drop all selected vertices which are not compatible with the conditions of a hierarchical support. By construction the remaining hierarchical support is the support of the best $\mathbf{s}$-sparse approximation in ℓ_2-norm to the input vector. The computational complexity of the general thresholding is $\mathcal{O}(d)$ as for the the standard s-sparse thresholding. Thus, the computation time of the most general HiHTP scales identically to the original HTP Algorithm.

In complete analogy to (s, σ)-sparse HiHTP, we can provide the following recovery guarantee for the general $\mathbf{s}$-sparse case.

Theorem 4 (Recovery guarantee)**.** *Suppose that the following RIP condition holds*

$$\delta_{3\mathbf{s}} < \frac{1}{\sqrt{3}}. \tag{19}$$

Given $\mathbf{x} \in \mathbb{C}^d$, $\mathrm{e} \in \mathbb{C}^m$, and an $\mathbf{s}$-sparse support $\boldsymbol{\Omega}$ on a tree T with associated vector support Ω, i.e., the set of indices of the active leaves of T. Then, the sequence $(\mathbf{x}^k)$ defined by HiHTP *(Algorithm 1) with thresholding operator $L_{\mathbf{s}}$ and $\mathbf{y} = \mathbf{A}\mathbf{x}\rfloor_\Omega + \mathbf{e}$ satisfies, for any $k \geq 0$,*

$$\left\|\mathbf{x}^k - \mathbf{x}\rfloor_\Omega\right\| \leq \rho^k \left\|\mathbf{x}^0 - \mathbf{x}\rfloor_\Omega\right\| + \tau \left\|\mathbf{e}\right\|, \tag{20}$$

where

$$\rho = \left(\frac{2\delta_{3\mathbf{s}}^2}{1 - \delta_{2\mathbf{s}}^2}\right)^{1/2} < 1 \tag{21}$$

and $\tau \leq 5.15/(1 - \rho)$.

As before we make use of the natural generalisation of RIP to the sparsity structure at hand to define $\mathbf{s}$-RIP constants $\delta_{\mathbf{s}}$ bounding $\|\mathbf{A}\mathbf{x}\|^2$ for all $\mathbf{s}$-sparse $\mathbf{x} \in \mathbb{R}^d$. In addition, for $q \in \mathbb{N}$ multiplication of $\mathbf{s}$ is defined pointwise as $q\mathbf{s}(v) \coloneqq \max\{q\mathbf{s}(v), n(v)\}$ for all $v \in V$.

The proof of Theorem 4 can be close to exactly copied from Theorem 1. The only required modification is a more general formulation of the Observation 2.

Given an arbitrary $\mathbf{s}$-sparse hierarchical support, the result of ref. [22] allows to provide a bound on $\delta_{\mathbf{s}}$ for measurement matrices with i.i.d. real Gaussian entries. To this end, the number $L = L(v_0)$ of $\mathbf{s}$-sparse hierarchical supports on T can be recursively calculate using

$$p(v) = \sum_{\substack{W \subset \operatorname{children}(v),\, w \in W \\ |W| = s(v)}} \prod p(w). \tag{22}$$

Since the resulting expression is not concise, we illustrate the generalised RIP bound with another important special case. Consider an $\mathbf{s}(v)$-sparse setting where all vertices of the depth i share a common number of children $n_i = \mathbf{n}(v)$ and sparsity $s_i = \mathbf{s}(v)$. The number of such supports of depth l is given by

$$L = \prod_{i=0}^{l} \binom{n_i}{s_i}^{s_{i-1}} \tag{23}$$

with the convention that $s_{-1} \coloneqq 1$. With (16) we therefore get the following generalised version of Theorem 3:

Theorem 5 (s-sparse RIP for real Gaussian measurements)**.** *Let* $\mathbf{A}$ *be an* $m \times (N \cdot n)$ *real matrix with i.i.d. Gaussian entries and* $m < Nn$*. For* $\epsilon > 0$*, assume that*

$$m \geq \frac{36}{7\delta}\left(\sum_{i=0}^{l} \mathbf{s}_{i-1} \ln\left(\frac{\mathrm{e}\,\mathbf{n}_i}{\mathbf{s}_i}\right) + \ln\left(\frac{12}{\delta}\right) + \ln(\epsilon^{-1})\right), \tag{24}$$

with $s_{-1} \coloneqq 1$*. Then, with probability of at least* $1-\epsilon$*, the restricted isometry constant* $\delta_{\mathbf{s}}$ *of* $\mathbf{A}/\sqrt{m}$ *satisfies*

$$\delta_{\mathbf{s}} \leq \delta. \tag{25}$$

More general $\mathbf{s}(v)$-sparse settings can be evaluated following the same strategy. However, the resulting expression for the number of samples m are in general more involved.

VI. Conclusion

We have demonstrated that the channel estimation task in multi-user machine-type communication setting amounts to the reconstruction of a vector with a simple instance of a hierarchical sparse structure, namely (s,σ)-sparsity. Furthermore, in a slightly simplified version of the CCRA protocol the measurement map can be regarded to be partial Fourier measurements. For the efficient recovery of (s,σ)-sparse vectors a variant of HTP algorithm, the HiHTP, was formulated. The HiHTP algorithm analytically and numerically proves itself more succesful in the recovery in terms of the sampling complexity compared to established compressed sensing methods. At the same time, it is computationaly not more expensive than the original HTP algorithm. The same strategy can be applied to the larger class of hierarchical sparse signals with multiple nested levels of groupings and different sparsities associated to each group.

It is also straight-forward to include a collaborative, jointly-sparse extension of the hierarchical sparse structure in the algorithm, where different copies or blocks of a signal have the same sparsity pattern. To this end, the thresholding operator has to be evaluated on the ℓ_2-norm of the entries that share the same sparsity structure. In this way, the slightly more general setting originally investigated in refs. [3], [5] can be incorporated in the HiHTP algorithm.

In this work, bounds on generalised RIP constants for hierarchical sparse structures were derived for Gaussian measurements. It is an interesting open question to find similar results for other measurement ensembles such as partial Fourier measurements. Especially, for an information theoretic analysis of the CCRA framework using HiHTP for the channel estimation task such results are of essential importance.

It is also an interesting further direction to identify recovery guarantees in the non-commutative analogous setting. The closest such setting is given by *tree tensor networks* [37] from quantum mechanics, which are also referred to by the name *hierarchical Tucker* tensor format [38], [39]. Very recently, a tensor version of the Iterative Hard Thresholding (IHT) algorithm [29] has been put forward covering this non-commutative analogue and already including partial recovery guarantees [40].

Appendix A
Proof of Theorem 1

For the proof of Theorem 1 we need a slightly more general formulation of some standard results abouts RIP constants to cover the case of (s,σ)-sparse RIP constants. We begin with the following simple statement, which is related to the common equivalent formulations of RIP constants [2, Chapter 6.1].

Proposition 6 (Equivalent characterizations of RIP)**.** *Let* $\Omega \subset [d]$ *be a support and* $\mathbf{A} \in \mathbb{K}^{m\times d}$ *be a measurement map. Then the following two statements are equivalent:*

1) $\delta \geq \|\mathrm{Id} - \mathbf{A}_\Omega^* \mathbf{A}_\Omega\|$,
2) $\forall \mathbf{x} \in \mathbb{K}^d$ *with* $\operatorname{supp}(\mathbf{x}) \subset \Omega$

$$(1-\delta)\,\|\mathbf{x}\|^2 \leq \|\mathbf{A}\mathbf{x}\|^2 \leq (1+\delta)\,\|\mathbf{x}\|^2 . \tag{26}$$

Proof: The inequality

$$\delta \geq \|\mathrm{Id} - \mathbf{A}_\Omega^*\mathbf{A}_\Omega\| = \max_{\mathbf{x}\in\mathbb{K}^d} \frac{|\,\langle \mathbf{x}, \mathbf{x} - \mathbf{A}_\Omega^*\mathbf{A}_\Omega(\mathbf{x})\rangle\,|}{\langle \mathbf{x},\mathbf{x}\rangle} \tag{27}$$

$$= \max_{\operatorname{supp}(\mathbf{x})=\Omega} \frac{|\,\langle \mathbf{x},\mathbf{x}\rangle - \langle \mathbf{A}\mathbf{x}, \mathbf{A}\mathbf{x}\rangle\,|}{\langle \mathbf{x},\mathbf{x}\rangle} \tag{28}$$

holds if and only if for all $\mathbf{x} \in \mathbb{K}^d$ with $\operatorname{supp}(\mathbf{x}) = \Omega$

$$\delta\,\langle \mathbf{x},\mathbf{x}\rangle \geq |\,\langle \mathbf{x},\mathbf{x}\rangle - \langle \mathbf{A}\mathbf{x},\mathbf{A}\mathbf{x}\rangle\,|. \tag{29}$$

The last bound is equivalent with (26). ∎

If a matrix satisfies RIP, then one can put a similar bound on its adjoint, which can be formalized as an obvious generalization of ref. [2, Lemma 6.20]:

Proposition 7 (Adjoint RIP)**.** *Let* $\Omega \subset [d]$ *be a support,* $\mathbf{A} \in \mathbb{K}^{m\times d}$ *be a measurement map and* $\mathbf{e} \in \mathbb{K}^d$ *a vector. If* $\|\mathrm{Id} - \mathbf{A}_\Omega^*\mathbf{A}_\Omega\| \leq \delta$ *then*

$$\|(\mathbf{A}^*\mathbf{e})_\Omega\| \leq \sqrt{1+\delta}\,\|\mathbf{e}\| . \tag{30}$$

Proof: We use that $\|\mathbf{x}_\Omega\| = \|\mathbf{x}\rfloor_\Omega\|$ and the Cauchy-Schwarz inequality to obtain

$$\|(\,\mathbf{A}^*\mathbf{e}\,)_\Omega\|^2 = \langle \mathbf{A}^*\mathbf{e}, (\mathbf{A}^*\mathbf{e})\rfloor_\Omega\rangle = \langle \mathbf{e}, \mathbf{A}\,(\mathbf{A}^*\mathbf{e})\rfloor_\Omega\rangle \tag{31}$$
$$\leq \|\mathbf{A}(\mathbf{A}^*\mathbf{e})\rfloor_\Omega\|\,\|\mathbf{e}\| .$$

Applying Proposition (6) yields

$$\|(\,\mathbf{A}^*\mathbf{e}\,)_\Omega\|^2 \leq \sqrt{1+\delta}\,\|(\,\mathbf{A}^*\mathbf{e}\,)_\Omega\|\,\|\mathbf{e}\| \tag{32}$$

and cancellation of the factor $\|(\,\mathbf{A}^*\mathbf{e}\,)_\Omega\|$ completes the proof. ∎

Next, we make an observation allowing to restrict the columns of a matrix.

Proposition 8 (Restricting columns)**.** *Let* $\mathbf{A} \in \mathbb{K}^{m\times d}$ *be a matrix,* $\mathbf{x} \in \mathbb{K}^d$ *a vector and* $\Omega \subset [d]$ *an index set. Then*

$$\left\|\left((\mathrm{Id} - \mathbf{A}^*\mathbf{A})\mathbf{x}\right)_\Omega\right\| \leq \left\|\mathrm{Id} - (\mathbf{A}_T)^*\mathbf{A}_T\right\|\,\|\mathbf{x}_T\|\,, \tag{33}$$

where $T = (\operatorname{supp}\mathbf{x}) \cup \Omega$.

The proof is analogous to the one presented in ref. [2, Lemma 6.16].

Proof: With $\mathbf{z} \coloneqq (\mathrm{Id} - \mathbf{A}^*\mathbf{A})\mathbf{x}$, $X \coloneqq \mathrm{supp}(\mathbf{x})$, and the definition of the projection onto support sets (7) we obtain

$$\begin{aligned}\left\|\left((\mathrm{Id} - \mathbf{A}^*\mathbf{A})\,\mathbf{x}\right)_\Omega\right\|^2 &= \left\langle \mathbf{z}\rfloor_\Omega, (\mathrm{Id} - \mathbf{A}^*\mathbf{A})\mathbf{x}\right\rangle && (34)\\ &= \left\langle \mathbf{z}\rfloor_\Omega, \mathbf{x}\right\rangle - \left\langle \mathbf{A}(\mathbf{z}\rfloor_\Omega), \mathbf{A}\mathbf{x}\right\rangle && (35)\\ &= \left\langle (\mathbf{z}\rfloor_\Omega)_T, \mathbf{x}_T\right\rangle - \left\langle \mathbf{A}_T\mathbf{z}_T, \mathbf{A}_T\mathbf{x}_T\right\rangle \\ &= \left\langle (\mathbf{z}\rfloor_\Omega)_T, \left(\mathrm{Id} - (\mathbf{A}_T)^*\mathbf{A}_T\right)\mathbf{x}_T\right\rangle \\ &\leq \|\mathbf{z}_\Omega\|\,\|\mathrm{Id} - (\mathbf{A}_T)^*\mathbf{A}_T\|\,\|\mathbf{x}_T\|. && (36)\end{aligned}$$

Cancelling the factor $\left\|\left((\mathrm{Id} - \mathbf{A}^*\mathbf{A})\,\mathbf{x}\right)_\Omega\right\| = \|\mathbf{z}_\Omega\|$ completes the proof. ∎

The proof requires a bound for terms involving sums of two and more (s,σ)-sparse vectors, to this end we will use the Observation 2 from Section III:

Observation (Support unions)**.** *For $i = 1, 2$ let $\Omega_i \subset [N] \times [n]$ be an (s_i, σ_i)-sparse support and $\mathbf{A} \in \mathbb{K}^{m\times Nn}$ with RIP constants $\delta_{s,\sigma}$. Then*

$$\left\|\mathrm{Id} - \mathbf{A}^*_{\Omega_1\cup\Omega_2}\mathbf{A}_{\Omega_1\cup\Omega_2}\right\| \leq \delta_{s_1+s_2,\sigma_1+\sigma_2}. \tag{37}$$

Now we are in the position to prove that HiHTP converges to the "right" solution for sufficiently many measurements.

Proof of recovery guarantee Theorem 1: We modify the argument as presented for HTP in ref. [2, Proof of Theorem 6.18]. Similar versions can be found in refs. [1] and [41]. The proof relies on two observations, that follow directly from the definition of the algorithm:

a) Consequence of Algorithm 1 Line 3: By definition, the thresholding operator $L_{s,\sigma}(\mathbf{z})$ yields the (s,σ)-sparse support such that $\left\|\mathbf{z}_{L_{s,\sigma}(\mathbf{z})}\right\| \geq \|\mathbf{z}_\Sigma\|$ for all (s,σ)-sparse $\Sigma \subset [Nn]$. In particular, Line 3 of Algorithm 1 ensures that in the $(k+1)^{\text{th}}$ iteration

$$\left\|\left(\mathbf{x}^k + \mathbf{A}^*(\mathbf{y} - \mathbf{A}\mathbf{x}^k)\right)_{\Omega^{k+1}}\right\| \geq \left\|\left(\mathbf{x}^k + \mathbf{A}^*(\mathbf{y} - \mathbf{A}\mathbf{x}^k)\right)_\Omega\right\|. \tag{38}$$

This bound still holds after eliminating the contribution of entries with indices in $\Omega \cap \Omega^{k+1}$. Hence,

$$\begin{aligned}&\left\|(\mathbf{x}^k + \mathbf{A}^*(\mathbf{y} - \mathbf{A}\mathbf{x}^k))_{\Omega^{k+1}\setminus\Omega}\right\| \\ &\quad\geq \left\|\left(\mathbf{x}^k + \mathbf{A}^*(\mathbf{y} - \mathbf{A}\mathbf{x}^k)\right)_{\Omega\setminus\Omega^{k+1}}\right\| \\ &\quad= \left\|\left(\mathbf{x}_\Omega - \mathbf{x}^{k+1} + \mathbf{x}^k - \mathbf{x}_\Omega + \mathbf{A}^*(\mathbf{y} - \mathbf{A}\mathbf{x}^k)\right)_{\Omega\setminus\Omega^{k+1}}\right\| \\ &\quad\geq \left\|\left(\mathbf{x}_\Omega - \mathbf{x}^{k+1}\right)_{\Omega\setminus\Omega^{k+1}}\right\| \\ &\qquad - \left\|\left(\mathbf{x}^k - \mathbf{x}_\Omega + \mathbf{A}^*(\mathbf{y} - \mathbf{A}\mathbf{x}^k)\right)_{\Omega\setminus\Omega^{k+1}}\right\|.\end{aligned} \tag{39}$$

This inequality can be recast as

$$\begin{aligned}&\left\|\left(\mathbf{x}_\Omega - \mathbf{x}^{k+1}\right)_{\Omega\setminus\Omega^{k+1}}\right\| \\ &\leq \left\|\left(\mathbf{x}^k - \mathbf{x}_\Omega + \mathbf{A}^*(\mathbf{y} - \mathbf{A}\mathbf{x}^k)\right)_{\Omega^{k+1}\setminus\Omega}\right\| \\ &\qquad + \left\|\left(\mathbf{x}^k - \mathbf{x}_\Omega + \mathbf{A}^*(\mathbf{y} - \mathbf{A}\mathbf{x}^k)\right)_{\Omega\setminus\Omega^{k+1}}\right\| \\ &\leq \sqrt{2}\left\|\left(\mathbf{x}^k - \mathbf{x}_\Omega + \mathbf{A}^*(\mathbf{y} - \mathbf{A}\mathbf{x}^k)\right)_{\Omega\Delta\Omega^{k+1}}\right\|,\end{aligned} \tag{40}$$

where $\Omega\Delta\Omega^{k+1} \coloneqq (\Omega \setminus \Omega^{k+1}) \cup (\Omega^{k+1} \setminus \Omega)$ denotes the symmetric difference of Ω and Ω^{k+1}.

b) Consequence of Algorithm 1 Line 4: The second observation is that, by definition, $\mathbf{x}^{k+1}$ calculated in Line 4 of Algorithm 1 fulfills the minimality condition

$$\left(\mathbf{A}^*(\mathbf{y} - \mathbf{A}\mathbf{x}^{k+1})\right)_{\Omega^{k+1}} = 0, \tag{41}$$

which can be seen by setting the gradient of $\mathbf{x} \mapsto \|\mathbf{A}\mathbf{x} - \mathbf{y}\|^2$ to zero.

With the bound (40) and the minimality condition (41) we are now in a position to find the bound

$$\begin{aligned}&\left\|\mathbf{x}_\Omega - \mathbf{x}^{k+1}\right\|^2 \\ &\quad= \left\|\left(\mathbf{x}^{k+1} - \mathbf{x}_\Omega\right)_{\Omega^{k+1}}\right\|^2 \\ &\qquad + \left\|(\mathbf{x}^{k+1} - \mathbf{x}_\Omega)_{\Omega\setminus\Omega^{k+1}}\right\|^2 \\ &\quad\leq \left\|\left(\mathbf{x}^{k+1} - \mathbf{x}_\Omega + \mathbf{A}^*(\mathbf{y} - \mathbf{A}\mathbf{x}^{k+1})\right)_{\Omega^{k+1}}\right\|^2 \\ &\qquad + 2\left\|\left(\mathbf{x}^k - \mathbf{x}_\Omega + \mathbf{A}^*(\mathbf{y} - \mathbf{A}\mathbf{x}^k)\right)_{\Omega\Delta\Omega^{k+1}}\right\|^2.\end{aligned} \tag{42}$$

Inserting $\mathbf{y} = \mathbf{A}\mathbf{x}_\Omega + \mathbf{e}$ yields

$$\begin{aligned}&\left\|\mathbf{x}^{k+1} - \mathbf{x}_\Omega\right\|^2 \\ &\quad\leq \Big[\left\|\left((\mathrm{Id} - \mathbf{A}^*\mathbf{A})(\mathbf{x}^{k+1} - \mathbf{x}_\Omega)\right)_{\Omega^{k+1}}\right\| \\ &\qquad + \left\|(\mathbf{A}^*\mathbf{e})_{\Omega^{k+1}}\right\|\Big]^2 \\ &\qquad + 2\Big[\left\|\left((\mathrm{Id} + \mathbf{A}^*\mathbf{A})(\mathbf{x}^k - \mathbf{x}_\Omega)\right)_{\Omega\Delta\Omega^{k+1}}\right\| \\ &\qquad\quad + \left\|(\mathbf{A}^*\mathbf{e})_{\Omega\Delta\Omega^{k+1}}\right\|\Big]^2.\end{aligned} \tag{43}$$

Using Proposition 8 and Lemma 2 we find for the first and third term that

$$\begin{aligned}&\left\|\left((\mathrm{Id} - \mathbf{A}^*\mathbf{A})(\mathbf{x}^{k+1} - \mathbf{x}_\Omega)\right)_{\Omega^{k+1}}\right\| \\ &\quad\leq \left\|\mathrm{Id} - \mathbf{A}^*_{\Omega\cup\Omega^{k+1}}\mathbf{A}_{\Omega\cup\Omega^{k+1}}\right\|\left\|\mathbf{x}^{k+1} - \mathbf{x}_\Omega\right\| \\ &\quad\leq c_1\left\|\mathbf{x}^{k+1} - \mathbf{x}_\Omega\right\|\end{aligned} \tag{44}$$

with $c_1 \coloneqq \delta_{2s,2\sigma}$ and

$$\begin{aligned}&\left\|\left((\mathrm{Id} + \mathbf{A}^*\mathbf{A})(\mathbf{x}^k - \mathbf{x}_\Omega)\right)_{\Omega\Delta\Omega^{k+1}}\right\| \\ &\quad\leq \left\|\mathrm{Id} - \mathbf{A}^*_{\Omega\cup(\Omega^{k+1}\setminus\Omega)\cup\Omega^k}\mathbf{A}_{\Omega\cup(\Omega^{k+1}\setminus\Omega)\cup\Omega^k}\right\|\left\|\mathbf{x}^k - \mathbf{x}_\Omega\right\| \\ &\quad\leq c_2\left\|\mathbf{x}^k - \mathbf{x}^\Omega\right\|\end{aligned} \tag{45}$$

with $c_2 \coloneqq \delta_{3s,2\sigma}$, where to accomplish the last step we notice that $\Omega \cup (\Omega^{k+1} \setminus \Omega)$ is $(2s,\sigma)$-sparse. For the remaining two terms Proposition 7 and Lemma 2 yield

$$\|(\mathbf{A}^*\mathbf{e})_{\Omega^{k+1}}\| \leq c_3\,\|\mathbf{e}\| \tag{46}$$

with $c_3 \coloneqq (1 + \delta_{s,\sigma})^{1/2}$ and

$$\|(\mathbf{A}^*\mathbf{e})_{\Omega\Delta\Omega^{k+1}}\| \leq \sqrt{1 + c_1}\,\|\mathbf{e}\|. \tag{47}$$

Plugging (44), (46), (45), (47) back into (43), solving the quadratic inequality for $\left\|\mathbf{x}^{k+1} + \mathbf{x}_\Omega\right\|$ and then using that

$\sqrt{a^2+b^2} \leq |a| + |b|$ for $a, b \in \mathbb{R}$ leads to

$$\begin{aligned}\left\|\mathbf{x}^{k+1} + \mathbf{x}_\Omega\right\| \leq & \left[\frac{2}{1-c_1^2}\left(c_2\left\|\mathbf{x}^k - \mathbf{x}_\Omega\right\| + \sqrt{1+c_1}\,\|\mathbf{e}\|\right)^2\right. \\ & \left. + \left(\frac{c_3}{1-c_1^2}\right)^2 \|\mathbf{e}\|^2\right]^{1/2} + \frac{c_1 c_3}{1-c_1^2}\|\mathbf{e}\| \\ \leq & \sqrt{\frac{2c_2^2}{1-c_1^2}}\left\|\mathbf{x}^k - \mathbf{x}_\Omega\right\| \\ & + \frac{\sqrt{2(1-c_1)}+c_3}{1-c_1}\|\mathbf{e}\|\,. \end{aligned} \tag{48}$$

We define $\rho := \sqrt{2c_2^2/(1-c_1^2)}$ and observe that

$$\rho \leq \sqrt{2c_2^2/(1-c_2^2)} < 1 \tag{49}$$

if $\delta_{3s,2\sigma} < 1/\sqrt{3}$. Furthermore, we define the parameter τ such that

$$(1-\rho)\tau = \frac{\sqrt{2(1-c_1)}+c_3}{1-c_1} \tag{50}$$

holds. In the regime $0 \leq c_1 \leq 1/\sqrt{3}$ we can make use of the linear bound

$$\frac{\sqrt{2(1-c_1)}+c_3}{1-c_1} \leq \sqrt{2} + c_3 + \lambda c_1 \tag{51}$$

with $\lambda = (4.733c_3 + 2.637)/2$. Plugging

$$c_3 \leq \sqrt{1+c_2} < \sqrt{1+1/\sqrt{3}} \tag{52}$$

and $c_1 \leq c_2 < 1/\sqrt{3}$ into the linear bound (51) yields

$$(1-\rho)\tau \leq 5.15, \tag{53}$$

which completes the proof. ■

Appendix B
Calibration of HiLasso

In the optimisation problem of the HiLasso algorithm

$$\text{minimise}\ \frac{1}{2}\|\mathbf{y} - \mathbf{A}\mathbf{x}\|^2 + \mu\|\mathbf{x}\|_{\ell_1} + \lambda\|\mathbf{x}\|_{\ell_2/\ell_1}. \tag{54}$$

the parameters μ and λ have to be choosen according to the sparsity structure of the signal and the noise level of the measurements.

In our tests the signals are $(s = 4, \sigma = 20)$-sparse with $N = 30$ blocks each of dimension $n = 100$. The support is drawn uniformly at random and the entries are i.i.d. real numbers drawn from a standard normal distribution. Figure 8 shows the percentage of recovered signals for different values of the parameters μ and λ of the HiLasso algorithm and different numbers m of noiseless Gaussian measurements. For each combination of μ and λ the algorithm is tested for 30 signals. A signal is recovered if it deviates by less than 10^{-5} in Euclidean norm from the original signal.

We observe for a number of measurements m between 300–350 that choosing non-zero values for both parameters yields recoveries while setting one parameter to zero, corresponding

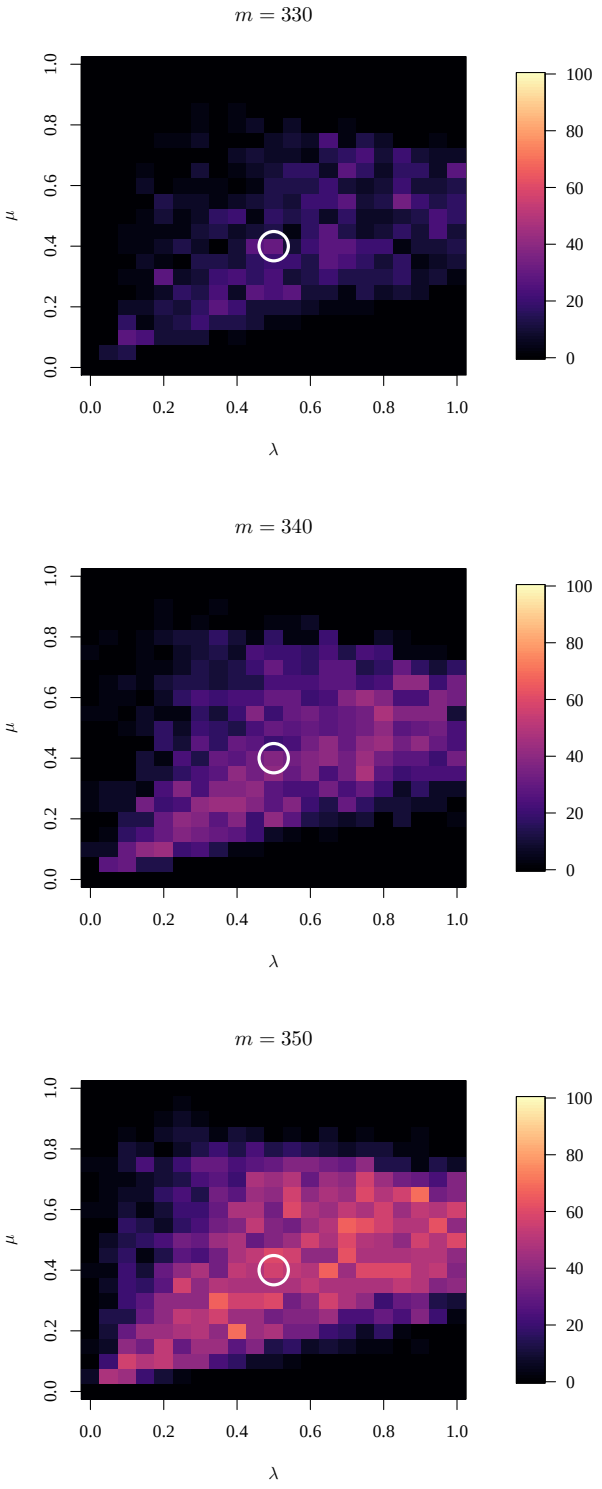

Figure 8. The three figures show the percentage of recovered signals for HiLasso using different calibration parameters μ and λ for numbers of measurements $m = 320$, $m = 340$ and $m = 350$, respectively. The value of $\mu = 0.4$ and $\lambda = 0.5$ used for Figure 2 and Figure 3 are highlighted by a white circle. The dimension of the signals are $N = 30$, $n = 100$, $s = 4$ and $\sigma = 20$

to standard ℓ_1-regularisation and mixed ℓ_1/ℓ_2-norm regularisation, does not.

For the numerics of Figure 2 and Figure 3 we choose the parameter $\mu = 0.5$ and $\lambda = 0.4$. This calibration point lies approximately in the center of the parameters for which recoveries are observed and is among the maximal points within the statistical error. In fact, using a couple of randomly selected further calibration points which appear reasonable form Figure 8 yield the same results for Figure 2 and Figure 3.

Acknowledgements

We thank A. Steffens, C. Riofrío and C. Krumnow for helpful discussions. We are also grateful to S. Kitić, P. Schniter and P. Boufounos for pointing to related references. The research of IR, MK, JE has been supported by the DFG project EI 519/9-1 (SPP1798 CoSIP), the Templeton Foundation, the EU (RAQUEL), the BMBF (Q.com), and the ERC (TAQ). The work of MK has also been supported by the Excellence Initiative of the German Federal and State Governments (Grant ZUK 81), the DFG (SPP1798 CoSIP), and the Polonez grant 2015/19/P/ST2/03001. The work of GW was carried out within DFG grants WU 598/7-1 and WU 598/8-1 (SPP1798 CoSIP), and the 5GNOW project, supported by the European Commission within FP7 under grant 318555.

References

[1] S. Foucart, "Hard thresholding pursuit: An algorithm for compressive sensing," *SIAM J. Num. An.*, vol. 49, pp. 2543–2563, 2011.

[2] S. Foucart and H. Rauhut, *A mathematical introduction to compressive sensing*. Springer, 2013.

[3] P. Sprechmann, I. Ramirez, G. Sapiro, and Y. Eldar, "Collaborative hierarchical sparse modeling," in *2010 44th Annual Conference on Information Sciences and Systems (CISS)*, 2010, pp. 1–6.

[4] J. Friedman, T. Hastie, and R. Tibshirani, "A note on the group lasso and a sparse group lasso," *arXiv:1001.0736 [math, stat]*, 2010, arXiv: 1001.0736.

[5] P. Sprechmann, I. Ramirez, G. Sapiro, and Y. C. Eldar, "C-HiLasso: A collaborative hierarchical sparse modeling framework," *IEEE Trans. Sig. Proc.*, vol. 59, pp. 4183–4198, 2011.

[6] N. Simon, J. Friedman, T. Hastie, and R. Tibshirani, "A sparse-group Lasso," *J. Comp. Graph. Stat.*, vol. 22, no. 2, pp. 231–245, 2013.

[7] P. Dighe, A. Asaei, and H. Bourlard, "Sparse modeling of neural network posterior probabilities for exemplar-based speech recognition," *Speech Communication*, vol. 76, pp. 230–244, 2016.

[8] M. Dao, N. H. Nguyen, N. M. Nasrabadi, and T. D. Tran, "Collaborative multi-sensor classification via sparsity-based representation," *IEEE Trans. Sig. Proc.*, vol. 64, pp. 2400–2415, 2016.

[9] H. Liu, Y. Yu, F. Sun, and J. Gu, "Visual-tactile fusion for object recognition," *IEEE Trans. Aut. Sc. Eng.*, vol. PP, pp. 1–13, 2016.

[10] Y. C. Eldar and M. Mishali, "Robust recovery of signals from a structured union of subspaces," *IEEE Trans. Inf. Th.*, vol. 55, no. 11, pp. 5302–5316, 2009.

[11] ——, "Block sparsity and sampling over a union of subspaces," in *Digital Signal Processing, 2009 16th International Conference on*, 2009, pp. 1–8.

[12] B. Adcock, A. C. Hansen, C. Poon, and B. Roman, "Breaking the coherence barrier: A new theory for compressed sensing," *arXiv preprint arXiv:1302.0561*, 2013.

[13] C. Li and B. Adcock, "Compressed sensing with local structure: uniform recovery guarantees for the sparsity in levels class," *arXiv preprint arXiv:1601.01988*, 2016.

[14] R. G. Baraniuk, V. Cevher, M. F. Duarte, and C. Hegde, "Model-based compressive sensing," *IEEE Trans. Inf. Th.*, vol. 56, no. 4, pp. 1982–2001, Apr. 2010.

[15] G. Wunder et al, "5GNOW: Non-orthogonal, asynchronous waveforms for future mobile applications," *IEEE Communications Magazine*, vol. 52, no. 2, pp. 97–105, 2014.

[16] F. S. et al, "Fantastic-5g: flexible air interface for scalable service delivery within wireless communication networks of the 5th generation," *Transactions on Emerging Telecommunications Technologies*, Jul. 2016.

[17] G. Wunder, H. Boche, T. Strohmer, and P. Jung, "Sparse Signal Processing Concepts for Efficient 5G System Design," *IEEE ACCESS*, Dec. 2015, to appear. [Online]. Available: http://arxiv.org/abs/1411.0435

[18] G. Wunder, P. Jung, and M. Ramadan, "Compressive random access using a common overloaded control channel," *ArXiv e-prints, appeared at IEEE GLOBECOM'15 (San Diego (USA, December 2015)*, Apr. 2015.

[19] P. P. G. Wunder, C. Stefanovic, "Compressive Coded Random Access for Massive MTC Traffic in 5G Systems," in *49th Annual Asilomar Conf. on Signals, Systems*, Pacific Grove, USA, Nov. 2015, invited paper.

[20] W. U. Bajwa, J. Haupt, A. M. Sayeed, and R. Nowak, "Compressed channel sensing: A new approach to estimating sparse multipath channels," *Proc. IEEE*, vol. 98, no. 6, pp. 1058–1076, 2010.

[21] H. Zhu and G. B. Giannakis, "Exploiting sparse user activity in multiuser detection," *IEEE Trans. Comm.*, vol. 59, pp. 454–465, 2011.

[22] T. Blumensath and M. E. Davies, "Sampling theorems for signals from the union of finite-dimensional linear subspaces," *IEEE Trans. Inf. Theory*, vol. 55, no. 4, pp. 1872–1882, Apr. 2009.

[23] A. Majumdar and R. K. Ward, "Fast group sparse classification," *Canadian Journal of Electrical and Computer Engineering*, vol. 34, no. 4, pp. 136–144, 2009.

[24] H. Liu and F. Sun, "Hierarchical orthogonal matching pursuit for face recognition," in *The First Asian Conference on Pattern Recognition*, 2011, pp. 278–282.

[25] F. Bach, R. Jenatton, J. Mairal, and G. Obozinski, "Structured sparsity through convex optimization," *Stat. Sc.*, vol. 27, pp. 450–468, 2012.

[26] R. Jenatton, J.-Y. Audibert, and F. Bach, "Structured Variable Selection with Sparsity-Inducing Norms," *J. Mach. Learn. Res.*, vol. 12, no. Oct, pp. 2777–2824, 2011.

[27] ——, "Structured variable selection with sparsity-inducing norms," *J. Mach. Learn. Res.*, vol. 12, no. Oct, pp. 2777–2824, 2011.

[28] D. Needell and J. A. Tropp, "CoSaMP: Iterative signal recovery from incomplete and inaccurate samples," *Appl. Comp. Harm. An.*, 2008.

[29] T. Blumensath and M. E. Davies, "Iterative thresholding for sparse approximations," *J. Four. An. App.*, vol. 14, pp. 629–654, 2008.

[30] W. Dai and O. Milenkovic, "Subspace pursuit for compressive sensing signal reconstruction," *IEEE Trans. Inf. Th.*, vol. 55, pp. 2230–2249, 2009.

[31] J. A. Tropp, "Greed is good: algorithmic results for sparse approximation," *IEEE Trans. Inf. Th.*, vol. 50, pp. 2231–2242, 2004.

[32] C. A. R. Hoare, "Algorithm 65: Find," *Commun. ACM*, vol. 4, pp. 321–322, 1961.

[33] E. J. Candes and T. Tao, "Decoding by linear programming," *IEEE Trans. Inf. Th.*, vol. 51, pp. 4203–4215, 2005.

[34] MATLAB version 8.5.0. (R2015a), "The MathWorks Inc." Natick, Massachusetts, 2015.

[35] M. Grant and S. Boyd, "CVX: Matlab software for disciplined convex programming, version 2.1," http://cvxr.com/cvx, Mar. 2014.

[36] M. ApS, *The MOSEK optimization toolbox for MATLAB manual. Version 7.1 (Revision 28).*, 2015.

[37] Y.-Y. Shi, L.-M. Duan, and G. Vidal, "Classical simulation of quantum many-body systems with a tree tensor network," *Phys. Rev. A*, vol. 74, Aug 2006.

[38] W. Hackbusch and S. KÃijhn, "A new scheme for the tensor representation," *Journal of Fourier Analysis and Applications*, vol. 15, no. 5, pp. 706–722, Oct. 2009.

[39] L. Grasedyck, "Hierarchical singular value decomposition of tensors," *SIAM Journal on Matrix Analysis and Applications*, vol. 31, no. 4, pp. 2029–2054, Jan. 2010.

[40] H. Rauhut, R. Schneider, and Z. Stojanac, "Low rank tensor recovery via iterative hard thresholding," Feb. 2016, arXiv:1602.05217.

[41] J.-L. Bouchot, S. Foucart, and P. Hitczenko, "Hard thresholding pursuit algorithms: Number of iterations," *App. Comp. Harm. An.*, 2016.